

**Figure S1, Related to Figure 1: High-throughput approaches reveal putative antiviral lncRNAs** (A-C) HBMEC were uninfected or infected with CHIKV or ZIKV at MOI 5 for 24h in three independent experiments and subjected to total RNA-seq. Displayed are (A) Heat maps depicting IFN responsive gene expression with  $\log_2$  fold change greater than 1, read cutoff of 50, and adjusted p value of less than 0.05 in CHIKV and ZIKV-infected cells. (B) Gene set enrichment (GSEA) plots of enriched signatures induced by CHIKV or ZIKV in HBMEC. Y-axis represents enrichment score (ES). (C) Pie charts indicating the percentage of significantly upregulated transcripts which are coding vs. noncoding. Exact transcript numbers are shown. (D) Schematic describing the screen pipeline: a predesigned RNAi library targeting 2200 lncRNAs was transfected into HBMEC and knockdown was allowed to proceed for 3 days. The cells were then infected with CHIKV-mKate at MOI 0.05 for 24h, fixed and immunostained for nuclei (Hoechst). Images were acquired using automated microscopy and the percentage of cells infected was quantified. The screen was performed in duplicate and statistically analyzed using Z scores. (E) The structure of the CHIKV-mKate virus used in the screen is shown. (F) Cell number was measured using Hoechst staining and automated microscopy and Z scores were calculated. Data points with  $Z < -2$  are highlighted in black and were removed from percent infection data shown in Figure 1B. The antiviral and proviral candidates from Figure 1B are highlighted in light blue and purple respectively. *ALPHA* is highlighted in dark blue. (G) siRNAs targeting the pro-mitotic *KIF11* and anti-apoptotic genes (siDEATH) were used as controls for RNAi efficiency within the screen. Cell number was measured by Hoechst staining and automated microscopy. (H) siRNAs targeting *ZAP* were included as a positive control for an antiviral effect. Percent infection was measured by automated microscopy. Data are presented as fold change relative to siCON.  $n=2-3$ ; RNA-seq data are displayed as  $\log_2$  fold change with  $p < 0.05$ . \*\*\*\* $p < 0.001$ ; error bars represent S.E.M.;  $n=2$ ; Statistical analyses were performed using one-way ANOVA with Dunnett correction for multiple comparisons (G), Student's (unpaired, two-tailed) *t* test (H).

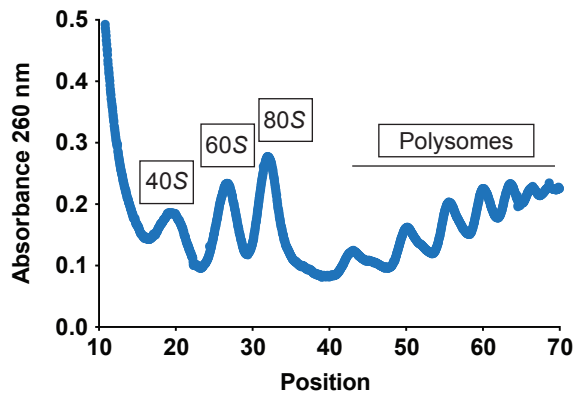
**A** Chromosome 21

100 kb

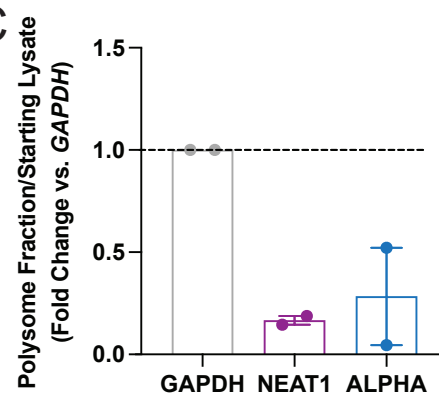
NCAM2

ENST00000452500  
(ALPHA)

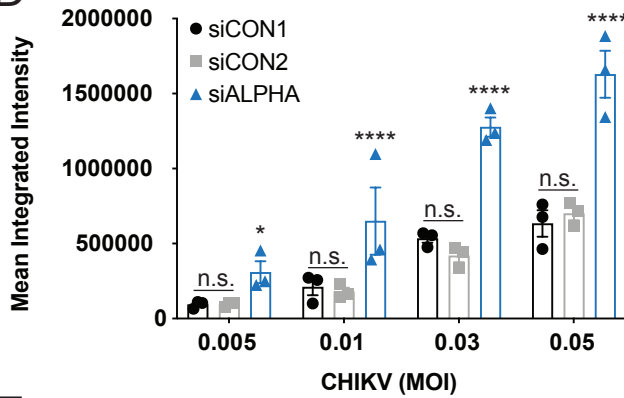
**B**



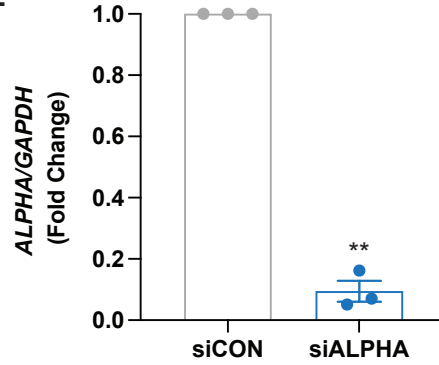
**C**



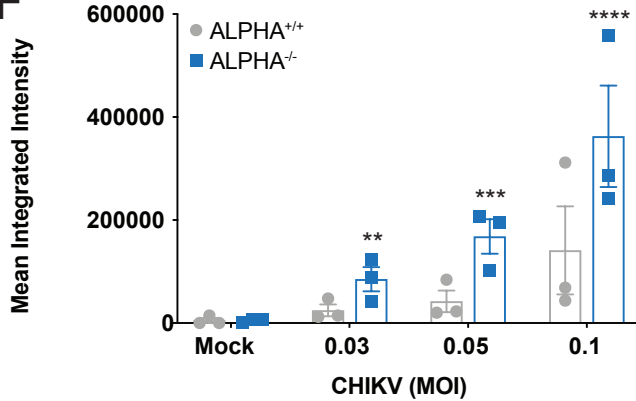
**D**



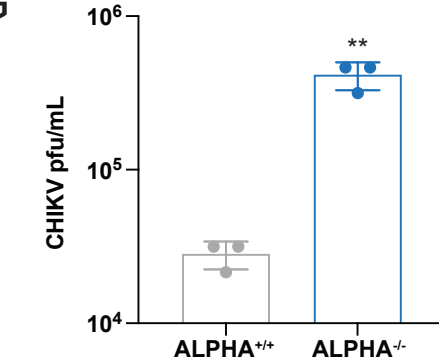
**E**



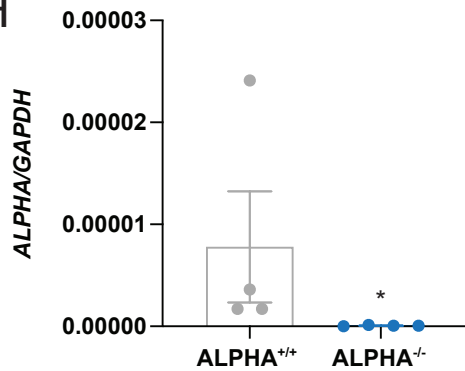
**F**



**G**



**H**



**I**

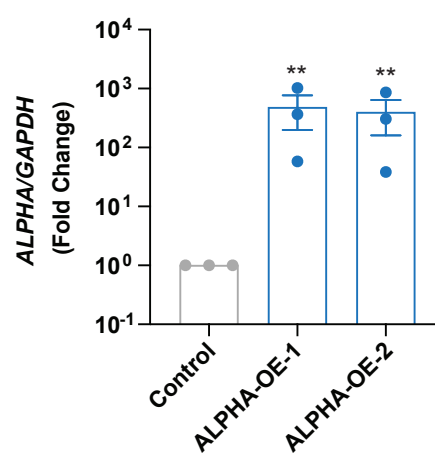


**Figure S2, Related to Figure 1: Characterization of *ALPHA* biology and function** (A) The *ALPHA* locus is encoded in Chromosome 21 and is comprised of 3 exons spanning 42 kb transcribed in the antisense direction relative to the nearest coding gene. The most proximal coding gene is neural cell adhesion molecule (NCAM)2 which is ~500 kb away. (B) Polysome fractions were isolated from HBMEC using a sucrose gradient and collected using a Biocomp Piston Gradient Fractionator. The y-axis refers to  $A_{260}$  absorbance values and the x-axis refers to fraction position. (C) RNA was isolated from either unfractionated total lysate or polysome fractions (positions 45-70) and *GAPDH*, *NEAT1*, and *ALPHA* were quantified by qPCR. *GAPDH* was used as a positive control for a translated mRNA and *NEAT1* was used as negative control for an untranslated ncRNA. Data are displayed as enrichment relative to total lysate. (D) *ALPHA* was depleted in HBMEC using pooled siRNAs and infected with CHIKV-mKate at the indicated MOIs for 24h. CHIKV protein was measured using immunofluorescence and automated microscopy. (E) Quantification of *ALPHA* in RNAi-depleted HBMEC by qPCR. (F-G) *ALPHA*<sup>+/+</sup> and *ALPHA*<sup>-/-</sup> HBMEC were (F) infected with CHIKV-mKate at the indicated MOIs for 24h and viral protein was quantified by immunofluorescence and automated microscopy or (G) infected with CHIKV MOI 0.2 for 30h and titers were quantified by TCID<sub>50</sub>. *ALPHA* levels in (H) *ALPHA*<sup>+/+</sup> and *ALPHA*<sup>-/-</sup> HBMEC and (I) control and *ALPHA* overexpressing HBMEC as measured by qPCR. Data in (I) are represented as fold change vs. control cells. *GAPDH* was used as a loading control in all qPCR experiments unless otherwise specified. \*p<0.05, \*\*p<0.01, \*\*\*p<0.001, \*\*\*\*p<0.0001; error bars are S.E.M.; n=2-4 as indicated; Statistical analyses were performed using two-way ANOVA with Sidak correction for multiple comparisons (D, F), Student's (unpaired, two-tailed) *t* test (E, G, H), one-way ANOVA with Dunnett correction for multiple comparisons (I).



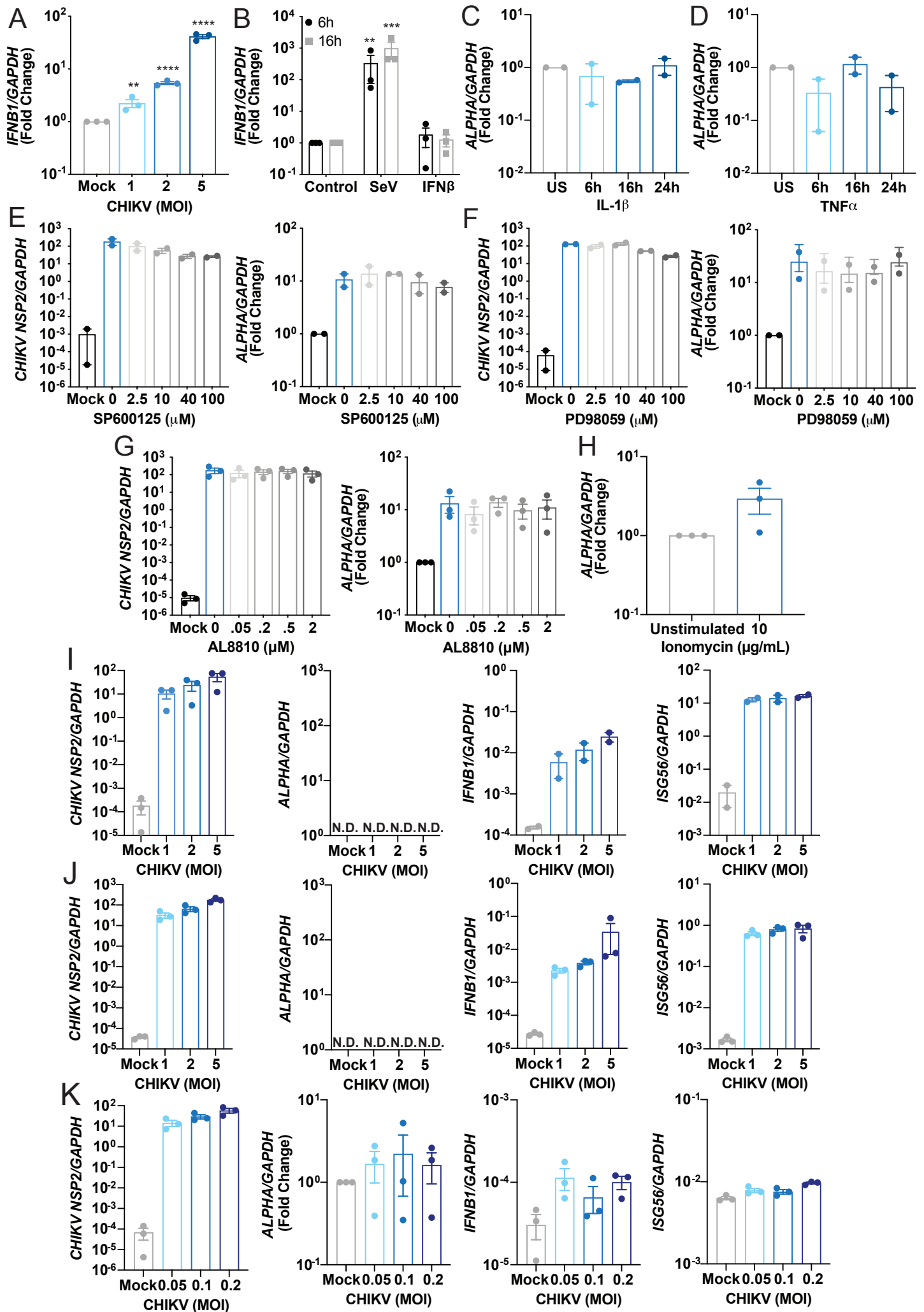


**Figure S3, Related to Figure 2: CHIKV-induced ALPHA upregulation is independent of classical signaling pathways and is cell type-specific** (A) HBMEC were infected with CHIKV for 24h at the indicated MOIs. *IFNB1* was measured by qPCR to assess activation of an innate immune response. Data are displayed as fold change vs. unstimulated cells. (B) HBMEC were treated with either Sendai virus (SeV, 100 HAU/mL) or recombinant IFN $\beta$  (10 ng/mL) for 6 or 16h and *IFNB1* was quantified by qPCR. Data are displayed as fold change vs. unstimulated cells. (C-D) HBMEC were stimulated with (C) IL-1 $\beta$  or (D) TNF $\alpha$  at 10 ng/mL for the indicated time points. *ALPHA* transcripts were measured by qPCR. Unstimulated cells are marked as US. (E-F) HBMEC were infected with CHIKV at MOI 5 for 24h and simultaneously treated with (E) SP600125 (JNK inhibitor) (F) PD98059 (MEK inhibitor) or (G) AL8810 (PGF $_{2\alpha}$  antagonist). CHIKV RNA and *ALPHA* were quantified in each of these experiments by qPCR. (H) Ionomycin (10  $\mu$ g/mL) was used to stimulate Ca $^{2+}$  signaling for 24h and *ALPHA* was quantified by qPCR. (I) Primary human peripheral blood monocytes, (J) A549 lung epithelial carcinoma cells, and (K) U2OS osteosarcoma cells were infected with CHIKV at the indicated MOIs for 24h. CHIKV RNA, *ALPHA*, *IFNB1*, and *ISG56* were quantified by qPCR. *ALPHA* expression is displayed as fold change relative to uninfected (mock) cells. *GAPDH* was used as a loading control in all experiments. \*\*p<0.01, \*\*\*p<0.001, \*\*\*\*p<0.0001; error bars are S.E.M.; n=2-3 as indicated; Statistical analyses were performed using one-way ANOVA with Dunnett correction for multiple comparisons (A, G), two-way ANOVA with Tukey correction for multiple comparisons (B), Student's (unpaired, two-tailed) *t* test (H).

**Fig S4**

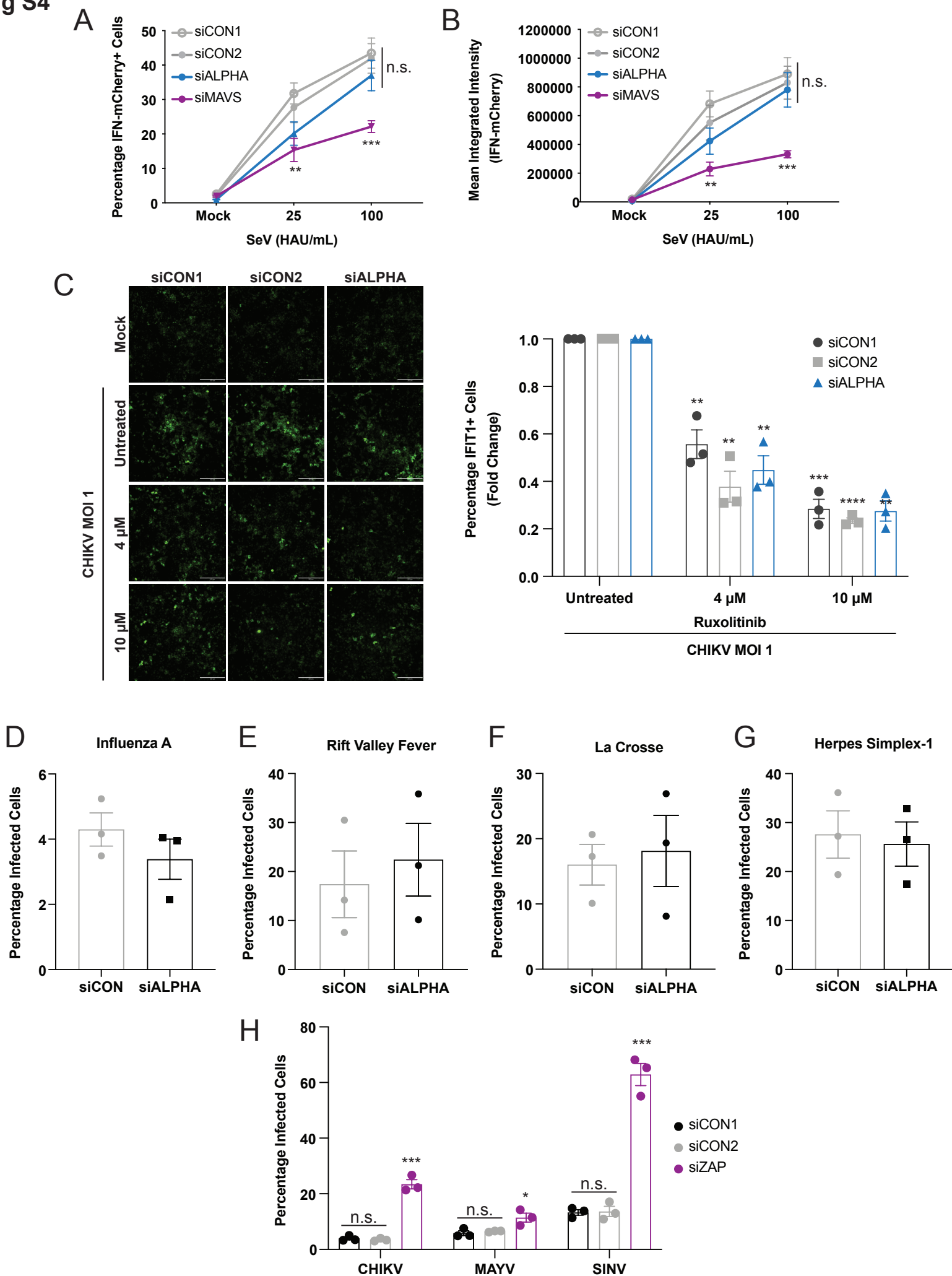


**Figure S4, Related to Figures 2 and 3: *ALPHA* activity is IFN-independent and virus-specific**

(A-B) HBMEC stably expressing an IFN-mCherry reporter were stimulated with SeV for 24h at the indicated concentrations following transfection with non-targeting siRNAs or siRNAs against *ALPHA* or *MAVS*. (A) Percent infection and (B) MFI were quantified by immunofluorescence and automated microscopy. (C) HBMEC were pre-treated for 2h with Ruxolitinib at the indicated concentrations followed by spin infection with CHIKV at MOI 1 for 24h. Representative images are shown (left). The percentage of IFIT1+ cells was quantified by immunofluorescence and automated microscopy (right). Data are displayed as fold change relative to the corresponding untreated control. Scale bars represent 200  $\mu$ m. (D-G) Control or *ALPHA*-depleted HBMEC were infected with (D) Influenza A (IAV, MOI 0.02), (E) Rift Valley Fever Virus (RVFV, MOI 0.01), (F) La Crosse Virus (LACV, MOI 0.01), or (G) Herpes Simplex Virus 1-GFP (HSV-1-GFP, MOI 0.005). The percentage of infected cells was quantified by immunofluorescence and automated microscopy. (H) Control or *ZAP*-depleted HBMEC were infected with CHIKV (MOI 0.03), MAYV (MOI 0.1), or SINV (MOI 0.1) for 24h. The percentage of infected cells was quantified by immunofluorescence and automated microscopy. \* $p < 0.05$ , \*\* $p < 0.01$ , \*\*\* $p < 0.001$ , \*\*\*\* $p < 0.0001$ ; error bars are S.E.M.;  $n = 3$ ; Statistical analyses were performed using two-way ANOVA with Tukey correction for multiple comparisons. Significance shown is relative to siCON1 (A, B), Student's (unpaired, two-tailed)  $t$  test with Holm-Sidak correction for multiple comparisons (C, H), Student's (unpaired, two-tailed)  $t$  test (D-G).

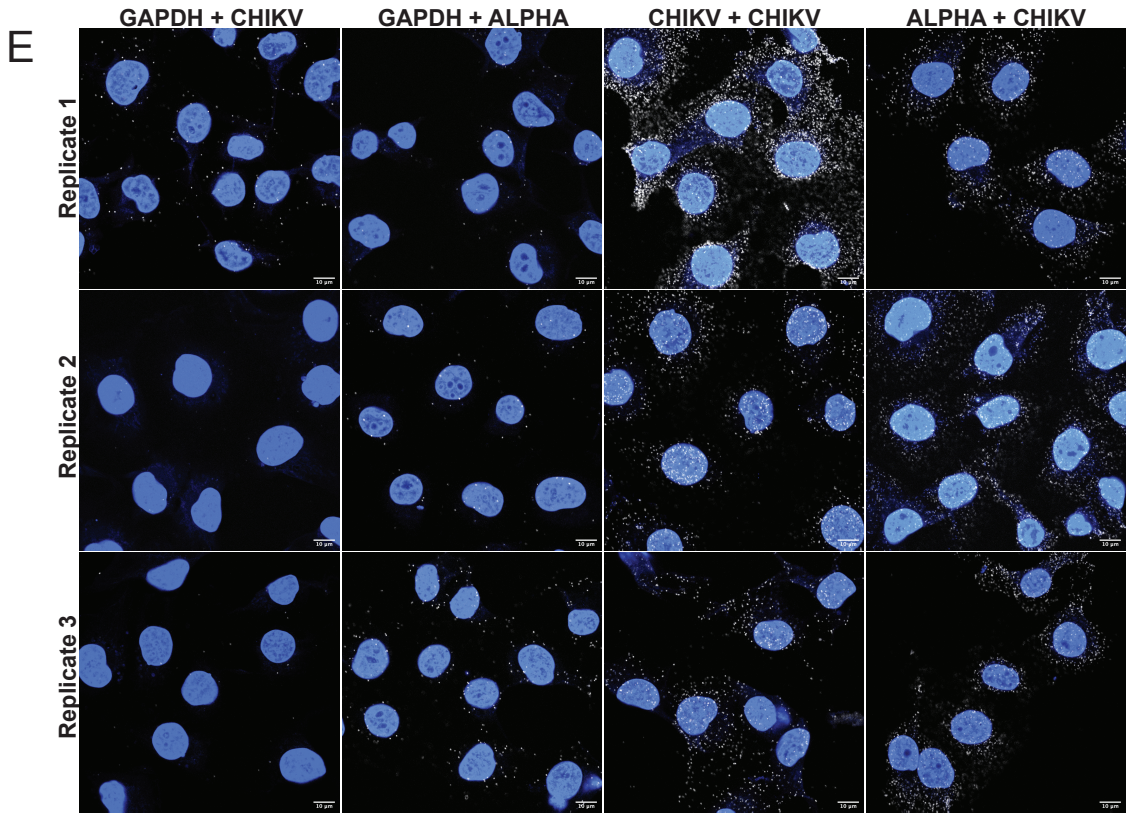
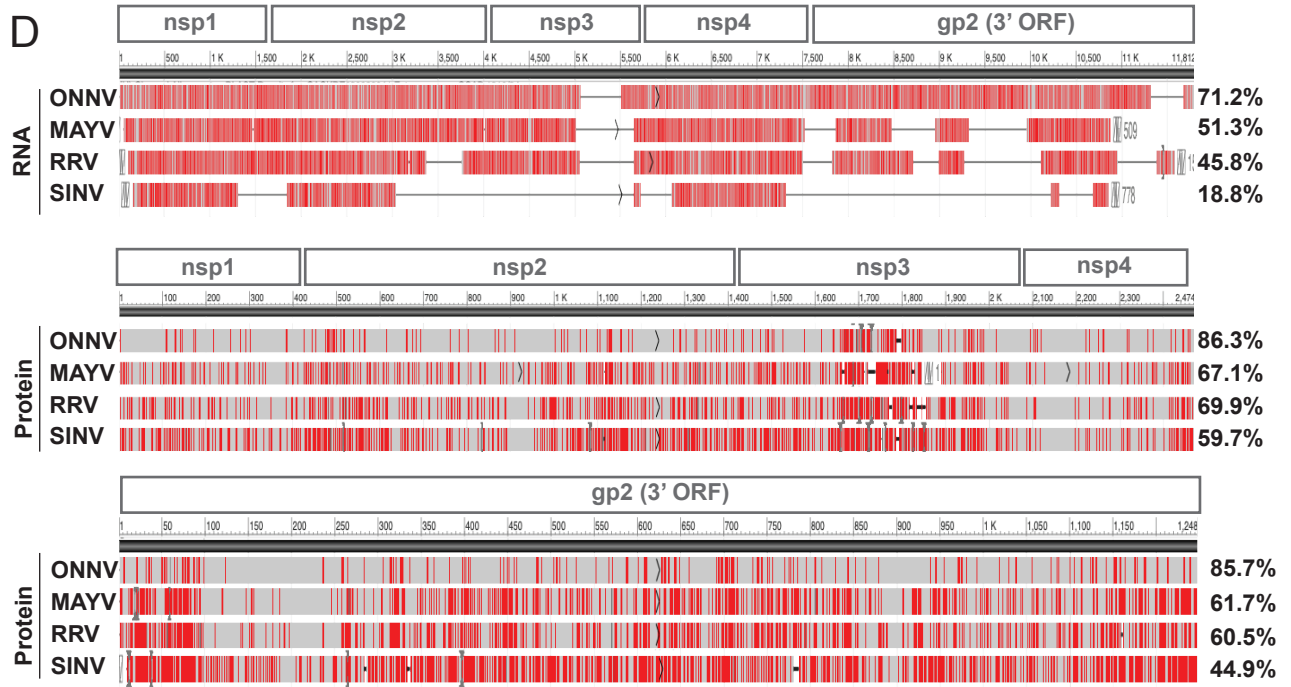
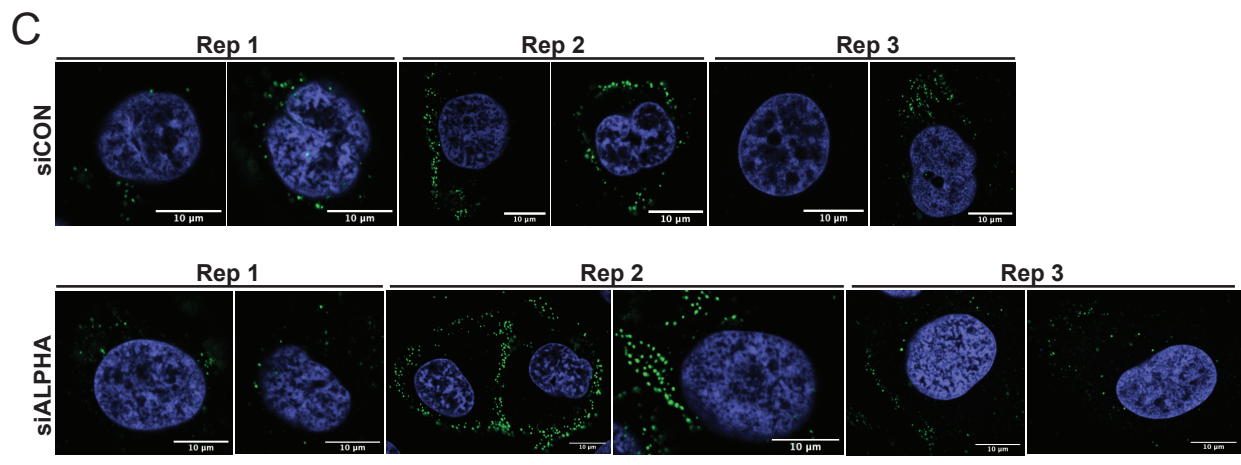
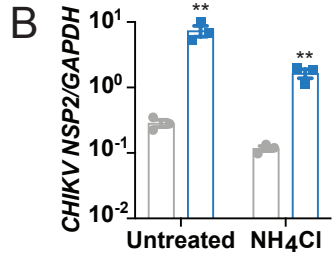
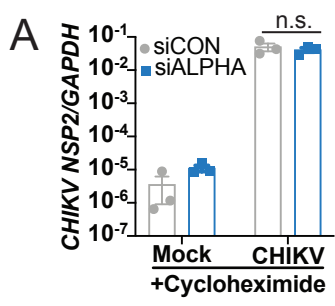


**Figure S5, Related to Figure 4: *ALPHA* does not regulate CHIKV entry or spread and interacts with CHIKV RNA in the cytoplasm** (A) Control and *ALPHA*-depleted HBMEC were infected with CHIKV at MOI 20 for 4h in the presence of cycloheximide (10  $\mu$ g/mL), extracellular virions were removed by trypsinization and intracellular CHIKV RNA was quantified by qPCR. (B) Control and *ALPHA*-depleted HBMEC were infected with CHIKV at MOI 0.05 for 4h followed by addition of either vehicle control or ammonium chloride ( $\text{NH}_4\text{Cl}$ ) for 24h. Viral RNA levels were quantified by qPCR. *GAPDH* was used as a loading control for (A) and (B). (C) Additional representative images for each independent experiment in Figure 4A are shown. Scale bars represent 10  $\mu$ m. (D) RNA and protein sequence alignments between related alphaviruses CHIKV (Ross), ONNV (SG650), MAYV (BeH407), RRV (T48), and SINV (Girdwood) generated using megaBLAST. The dark gray line at the top represents the CHIKV Ross reference sequence. Light gray rectangles represent regions of detected homology. Red lines demarcate nucleotides or amino acids which differ from CHIKV Ross. Thin black horizontal lines represent regions where there is no detectable homology. Percent identity compared to CHIKV Ross is indicated on the left. (E) HBMEC were infected with CHIKV at MOI 5 for 24h and subjected to PLA. Additional images corresponding to main Figure 4C-D from all three replicates are shown. Scale bars represent 10  $\mu$ m. \*\* $p < 0.01$ ; error bars are S.E.M.;  $n=3$ ; Statistical analyses were performed using two-way ANOVA with Sidak correction for multiple comparisons (A), Student's (unpaired, two-tailed) *t* test with Holm-Sidak correction for multiple comparisons (B).

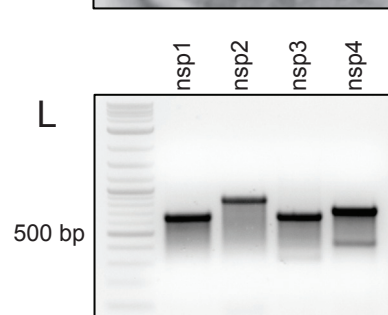
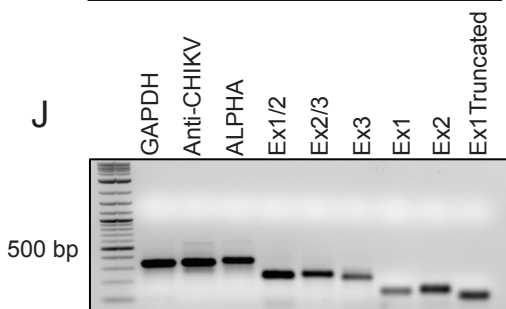
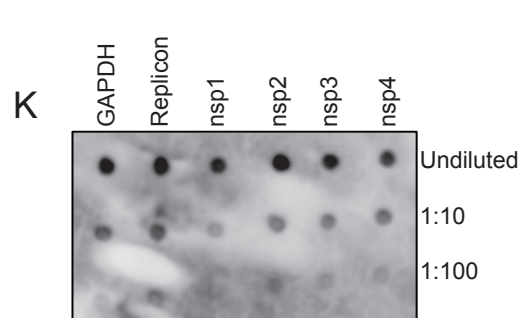
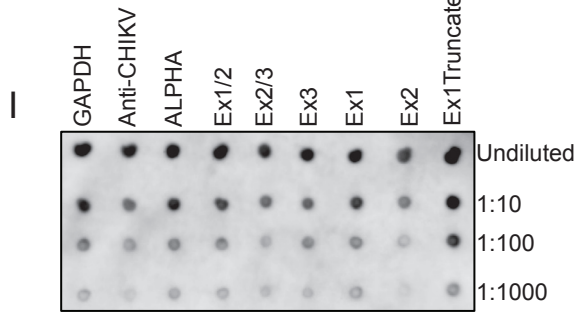
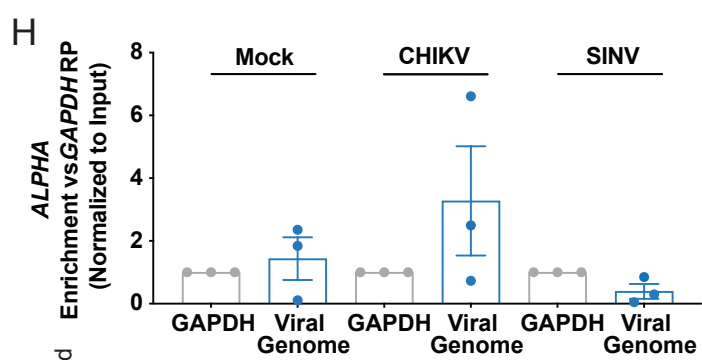
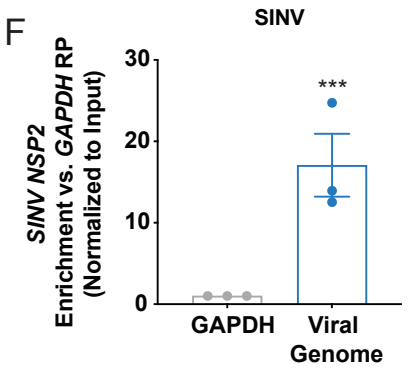
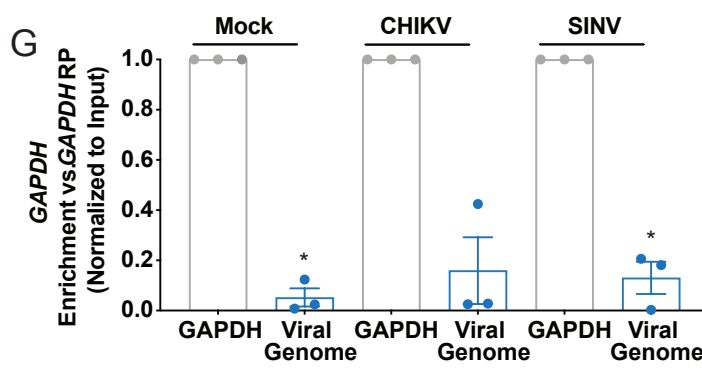
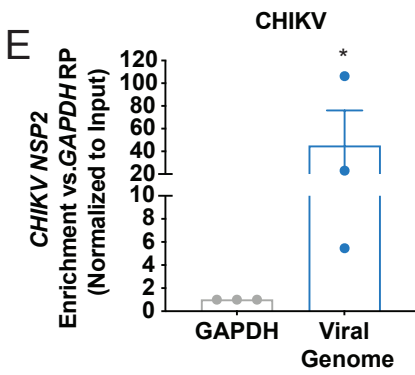
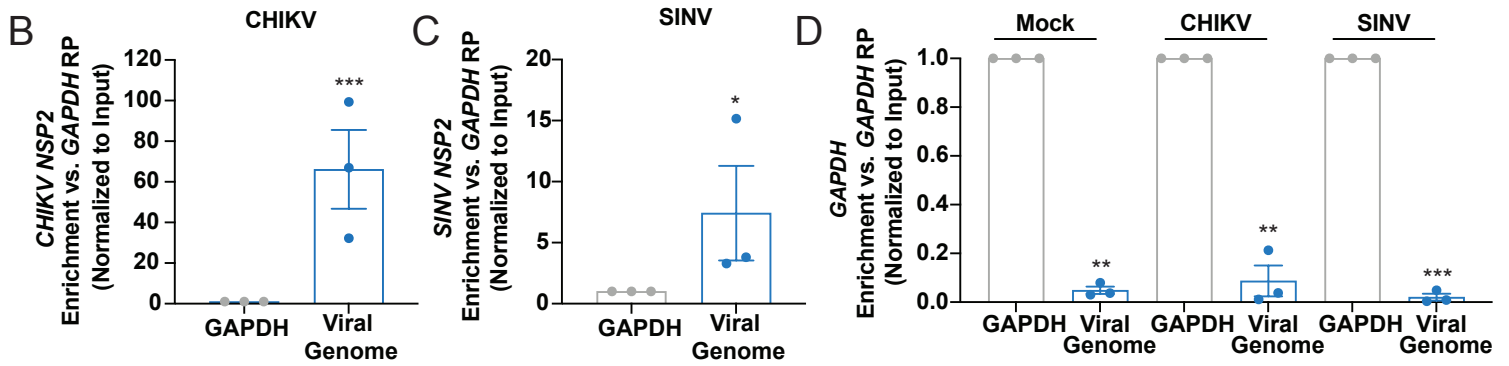
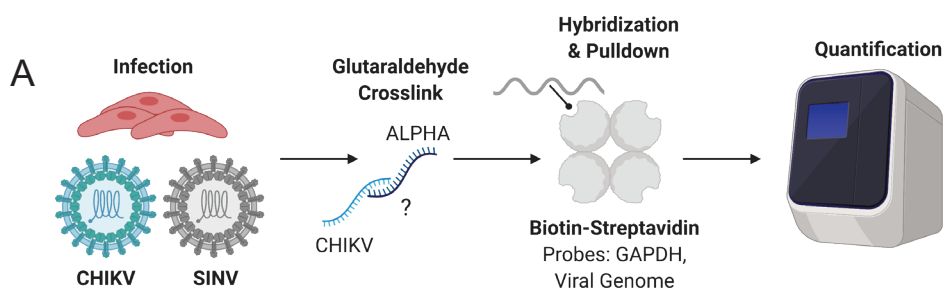
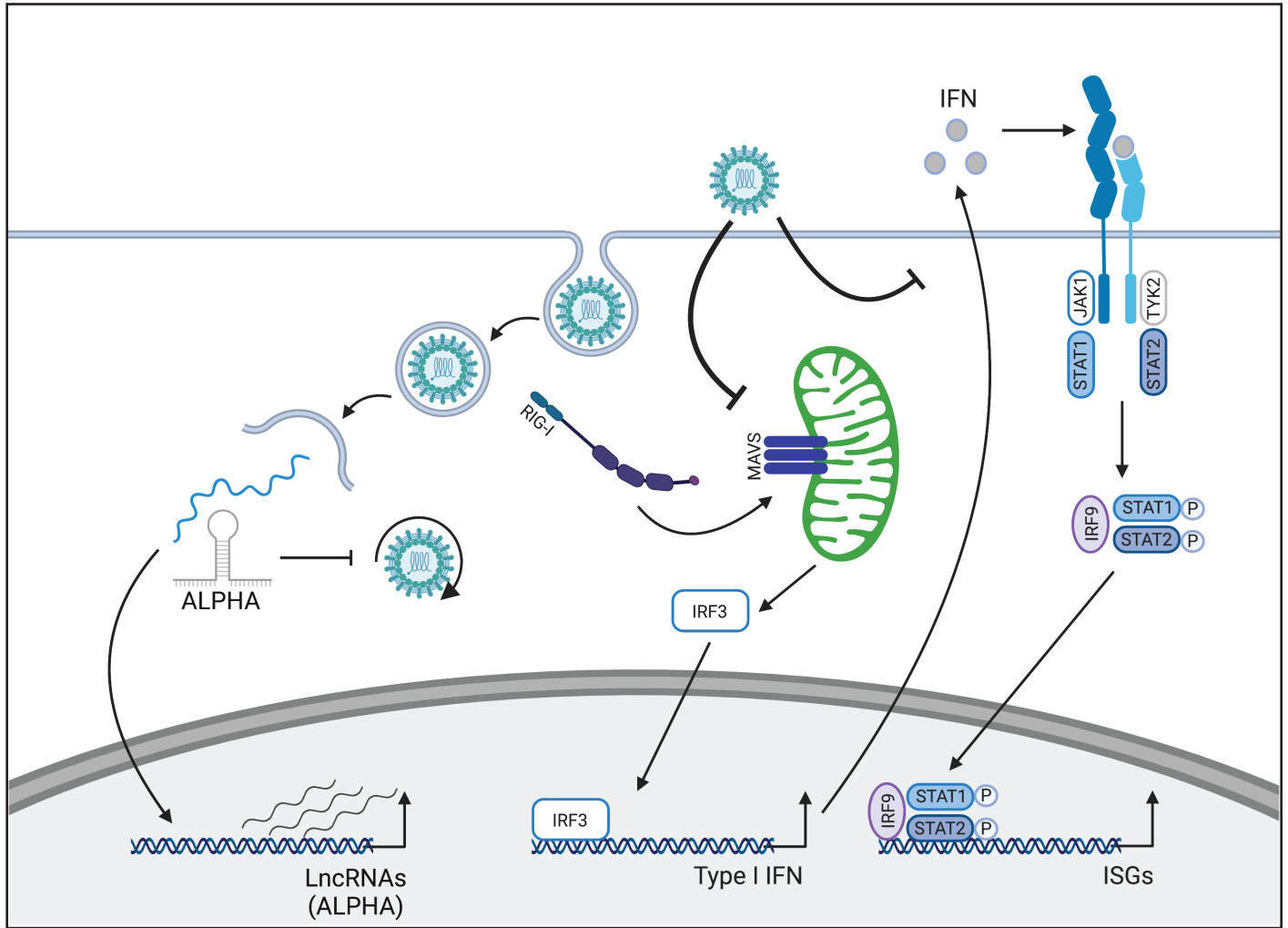




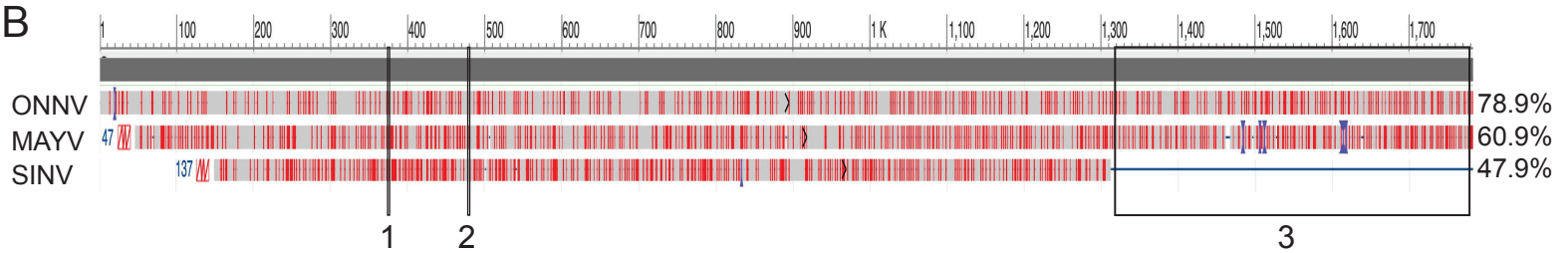
**Figure S6, Related to Figures 4 and 5: *ALPHA* interacts with CHIKV RNA in cells and *in vitro*** (A) *ALPHA*-overexpressing HBMEC were left uninfected or infected with either CHIKV and SINV and crosslinked with glutaraldehyde. Lysates were generated and hybridized with 500mer, biotinylated, antisense, oligonucleotide probes followed by enrichment with streptavidin-conjugated beads. The relative enrichment of (B) CHIKV RNA, (C) SINV RNA, and (D) *GAPDH* were measured by qPCR. (E-H) Wildtype HBMEC were uninfected or infected with CHIKV or SINV and crosslinked with glutaraldehyde. Lysates were generated and hybridized with 500mer, biotinylated, antisense, oligonucleotide probes followed by enrichment with streptavidin-conjugated beads. The relative enrichment of (E) CHIKV RNA, (F) SINV RNA, (G) *GAPDH*, and (H) *ALPHA* were measured by qPCR. (I) Streptavidin dot blot demonstrating the relative biotinylation levels of each RNA used in the *in vitro* RNA interaction assays shown in Figure 5B-D. 200 ng of each RNA was spotted in the top row and diluted as indicated. (J) Agarose gel showing the sizes of each RNA used in the *in vitro* RNA interaction assays shown in Figure 5B-D. 1.5  $\mu$ g of each RNA was visualized. (K) Streptavidin dot blot demonstrating the relative biotinylation levels of each RNA used in the *in vitro* RNA interaction assays shown in Figure 5E-F. 500 ng of replicon was used. Equal molar ratios relative to the replicon RNA were used for the remaining RNAs and diluted as indicated. (L) Agarose gel showing the sizes of each individual nsp RNA used in the *in vitro* RNA interaction assays shown in Figure 5E-H. 2.5  $\mu$ g of each RNA was visualized. \* $p < 0.05$ , \*\* $p < 0.01$ , \*\*\* $p < 0.001$ ; error bars are S.E.M.;  $n = 3$ ; Statistical analyses were performed using Student's (unpaired, two-tailed) *t* test (B, C, E, F), one-way ANOVA with Sidak correction for multiple comparisons (D, G, H).



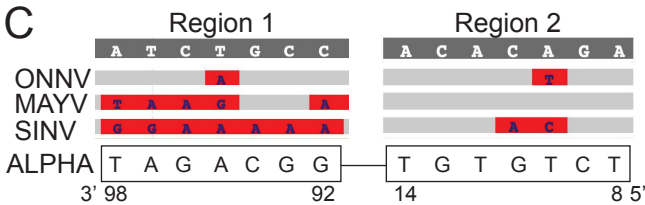
A



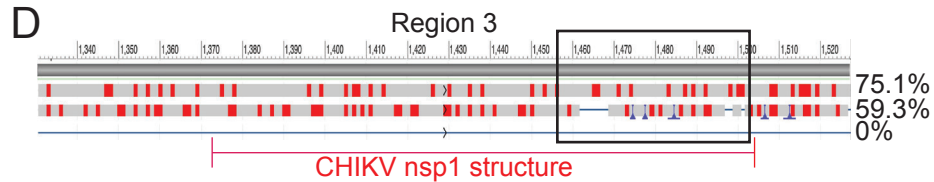
B



C

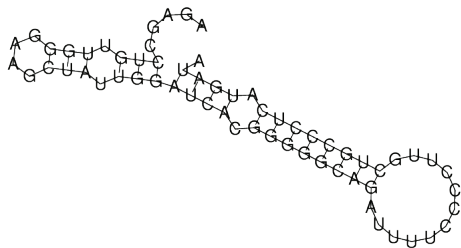


D



E

ALPHA ex1



F

ALPHA ex1 Truncated

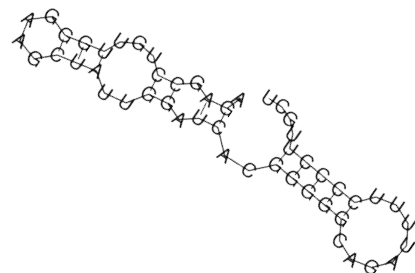


**Figure S7, Related to Figure 5 and Discussion: The functional role of *ALPHA* in innate immunity against CHIKV.** (A) Schematic illustrating *ALPHA*'s antiviral function against CHIKV. CHIKV infection results in the activation of classical innate signaling pathways including IFN. However, this response is antagonized by CHIKV. In parallel, many lncRNAs are induced by CHIKV including *ALPHA*, which localizes to the cytoplasm and directly interacts with CHIKV genomic RNA to prohibit viral replication independently of IFN. (B-D) Genomic alignments of the nsp1 gene between related alphaviruses using megaBLAST. (B) Full-length nsp1 is shown with black boxes demarcating putative *ALPHA* binding regions: 1) nucleotides 380-386, 2) nucleotides 484-490, and 3) the 3' end of nsp1. (C) Zoomed in schematics of regions 1 and 2. The complementary sequence withing the *ALPHA* sequence is detailed in the black boxes in the 3' to 5' direction with nucleotide numbers indicated (D) Zoomed in schematic of region 3. The structural element described in Madden, et al. between nucleotides 1377-1506 is demarcated by a red line. Gaps in the MAYV genome are indicated by black lines and highlighted by a black box. (E-F) Secondary structure predications generated using RNAfold for (E) full-length *ALPHA* ex1 and (F) truncated *ALPHA* ex1.